Biosurfactant assisted degradation of High Molecular Weight Polycyclic Aromatic Hydrocarbons by mixed cultures from a car service oil dump from Pretoria Central Business District (South Africa)

Evans M. Nkhalambayausi Chirwa[*], Tshilidzi B. Lutsinge-Nembudani, Oluwademilade M. Fayemiwo, Fisseha A. Bezza

Water Utilisation and Environmental Engineering Division, Department of Chemical Engineering, University of Pretoria, Pretoria, 0002, South Africa

ARTICLE INFO

ABSTRACT

Biomineralisation of polycyclic aromatic hydrocarbons (PAHs) and other toxic organic pollutants to CO_2 and H_2O is one of the most environmentally friendly and economically efficient options for treatment of deleterious organic pollutants in water and soil. Although most intermediate and high molecular weight (I-, HMW) PAHs are biodegradable, the degradability of these PAHs is limited by their low solubility. Experiments were conducted in batch reactors, and later, in continuous flow fixed-film bioreactor systems to take advantage of mass-transport resistance to reduce toxicity exposure within the biofilm. The results from this study showed a tenfold performance improvement in cumulative removal of PAHs in the biofilm reactor system. The active microbial agents were predominated by *Pseudomonas aeruginosa* MS-1 and Acinetobacter species. 98%, 88%, and 63% degradation of fluoranthene, pyrene and chrysene was achieved in the biofilm process, respectively, at steady doses of 45 kg/d fluoranthene, 12 kg/d pyrene and 7.5 kg/d chrysene, respectively. Product purification was further evaluated in a continuous flow fed-batch and plug-flow reactor system in which a high quality oil product was separated from oily sludge.

© 2020 Elsevier Ltd. All rights reserved.

1. Introduction

PAHs originate from both anthropogenic sources such as paint, detergents, medical and cosmetic products, pesticides and petrochemical effluents (Abdel-Shafy and Mansour, 2016; Cachada et al., 2018, 2019), and natural sources such as volcanism, forest fires and decaying plant matter (Lasota and Błońska, 2018; Malá et al., 2013). Previous studies showed that natural organic materials (NOMs) such as humic and fulvic acids, and compounds released by modern vegetation and fossilized plants can serve as parent materials for a range of PAHs (Lasota and Błońska, 2018; Zhong et al., 2017; Li et al., 2011). Breakdown compounds of multi-ring breakdown products of natural compounds resulting from vegetation decay such as humic and fulvic acid, for example, can react with chlorides and other halides to produce precursors of highly toxic and carcinogenic halogenated congeners of PAHs that have the ability to disrupt DNA replication causing increases in carcinogenesis and melanomas in mammalian life forms (Singer 1999).

In other studies, it was shown that a slew of PAH compounds can be released continuously from complex heterogeneous man-made compounds such as creosote and coal tar (Bezza and Chirwa, 2016). The reservoir in this case makes difficult to determine the effect PAH loading on the ecosystem due different solubilities of the different PAH components in the source material.

PAHs and their chlorinated congeners are notoriously resistant to degradation in the environment mainly due to their hydrophobicity and low solubility (Gan et al., 2009; Tudoran and Putz, 2012; Ukiwe et al., 2013). Several physical, chemical and biological methods have been considered to achieve biodegradation and overall remediation of PAH compounds. Examples of technologies tested include incineration (Chen et al., 2013; Sato et al., 2011; Wheatley and Sadhra, 2004), excavation and landfilling (Das and Chandran, 2011; Vidali, 2001), and land-farming (Bamforth and Singleton, 2005; Vidali, 2001). However, these treatment options were shown to be extremely expensive, difficult to execute, and

* Corresponding author.
E-mail addresses: evans.chirwa@up.ac.za, emnchirwa@gmail.com (E.M. Nkhalambayausi Chirwa).

inefficient when applied to large areas of contaminated land (Banat, 1995; Das and Chandran, 2011; Vidali, 2001).

On the other hand, organisms isolated from PAH contaminated environments show the potential to resist and degrade PAHs as primary carbon sources (Patowary et al., 2015). Cultures from these environments can be enriched and grown under biosurfactant producing environments, followed by introduction of the bio-surfactant as a separate dissolution agent to enhance the biode-gradability of the PAH compounds (Benincasa, 2007).

PAHs in complex matrices such as oil sludge could be selectively degraded while leaving behind the valuable shorter chain hydro-carbons critical in energy production (Dhote et al., 2010; Sarma et al., 2004). Such a processes was utilised previously by Chirwa et al. (2013) whereby a PAH degradation step was utilised as a clean-up step during oil recovery from storage tank sludge in batch systems. The process was recently included in an electro-osmotic oil recover study from petroleum contaminated soil in which live biosurfactant producing organisms were included in the process to recover a PAH free oil from the contaminated soil (Gidudu and Chirwa, 2019, 2020a, 2020b). The selective biodegradation ability of certain bacterial consortia have been utilised in the purification of oil separated from sludge using biosurfactants as demulsifying agents (Chirwa et al., 2013; Fayemiwo, 2015). The advantage of utilising whole culture biosurfactant generation systems over chemical demulsifiers is that, some of the cultures have an affinity for PAHs which they use as preferred carbon sources for growth and cell maintenance (Chang et al., 2015; Marchut-Mikolajczyk et al., 2018). In this study, the highest performing system with respect to oil recovery from oily sludge was achieved in a continuous-flow fed-batch system using biosurfactant-producing/PAH-degrading bacteria isolated from soil collected around an engine oil dump site in the Pretoria Central Business District (Pretoria CBD), in Gauteng (South Africa) (Fayemiwo, 2015; Chirwa et al., 2017, 2018).

The present study is aimed at enhancing the degradation of intermediate I- to HMW-PAHs under high biosurfactant production rate by taking advantage of the mass transport resistance in biofilm layers. The study sets out to find a biological culture capable of degrading IMW- to HMW-PAHs with the first ever demonstration of its feasibility in cleaning up PAH contaminated recovered oil from a complex matrix such as oily sludge. This was investigated using fluoranthene, pyrene and chrysene as model compounds. Mixed cultures from engine oil contaminated environments were used for the degradation of a range of PAHs in a preliminary study. For this particular study, a pure culture of the known PAH degrader, *Pseudomonas aeruginosa* MS-1, was used as a catalyst based on reported performance of the culture under mesophilic conditions.

2. Materials and methods

2.1. Culture and media

The mixed cultures of biosurfactant producing and PAH degrading bacteria used in this study were isolated from contam-inated soil collected from an oil dump site at a car service garage in Pretoria West (Pretoria, South Africa). The site was chosen due to a high probability of cultures that could be resilient to petrochemical pollution some of which could use these compounds as carbon sources and electron donors for life supporting metabolic pro-cesses. Stock cultures were prepared by adding 5 g of soil samples from the sites to 100 mL in three separated sterilized batches containing (1) nutrient broth (NB), (2) Luria-Bettani (LB) broth, and (3) MacConkey broth (MB), respectively. Suspended growth re-actors were supplied with Mineral Salts Medium (MSM) containing (in 1 L of deionised water): 6.0 g $(NH_4)_2SO_4$, 0.4 g $MgSO_4.7H_2O$, 0.4 g $CaCl_2.2H_2O$, 7.8 g $Na_2HPO_4.2H_2O$, 4.5 g KH_2PO_4 and 2 mL of trace

element solution. Trace element solution (L^{-1}) contained: 50 μM $CaCl_2$, 25 μM $FeSO_4$, 0.1 μM $ZnCl_2$, 0.2 μM $CuCl_2$, 0.1 μM NaBr, 0.05 μM Na_2MoO_2, 0.1 μM $MnCl_2$, 0.1 μM KI, 0.2 μM H_3BO_3, 0.1 μM $CoCl_2$, and 0.1 μM $NiCl_2$, and a carbon source of choice containing different dosed of cooking oil as starter medium for the biosurfactant for-mation. The flasks were then incubated at 37 °C for 42 h under continuous shaking at a rotary speed of 150 rpm. Growth of cells was evidenced by increased cloudiness of the broth (Rice et al., 2005).

2.2. Drop Collapse test

Different pure culture colonies grown on Nutrient, Luria-Bettani and McConkey agar were individually picked and tested for their ability to produce biosurfactants using the standard 'Drop Collapse' test (Bodour and Miller-Maier, 1998). The 'Drop Collapse' test is a qualitative method which utilises a 96-micro well plate coated with mineral oil. A 5 μL droplet of a water containing the test bacteria (approximately 10^5 cells in 5 μL) was delivered into the center of the well coated with oil using a pipette. A stable bead that might have formed in the absence of biosurfactants would collapse in the presence of a biosurfactant in the medium. Depending on the amount and effectiveness of the biosurfactant molecules, the droplet will either spread or collapse completely on the oil covered surface. If the droplet collapses or spreads out, it indicates the presence of a biosurfactant and if the droplet remains beaded up, it indicates the absence of the surfactants. A colouring reagent, in our case methyl blue, was added for ease of visualisation and for clear photographic imaging of the droplet (Shokouhfard et al., 2015).

2.3. Species identification by 16S rRNA genotype fingerprinting

Culture surviving the harsh pollution conditions were first pu-rified by multiple culturing on Nutrient Agar, Luria-Bettani Agar, and Universal Plate Agar to target specific species in the original consortium. Pure cultures of bacteria were grown from carefully wire-picked material from individual colonies on solid agar media. The picked material was re-suspended in sterile LB broth spiked with 10−15 mg/L of fluoranthene, pyrene and chrysene to ensure culture tolerance to target pollutants, and incubated until growth was observed. In order to increase culture purity, the batches from each identifiable colony were re-cultivated and purified until no contamination was observed in separate petri dishes. The Wizard Genomic DNA purification kit (Promega Corporation, Madison, WI, USA located at the University of Pretoria − Department of Micro-biology and Plant Pathology − was used to extract and purify DNA for further processing in the next stage. Special primers pA and pH1 were developed to target the position 8−27 (pA) and the position 1541−1522 (pH1) of the 16S gene sequence. The sequencing was conducted for 1 min at 94 °C, 30 cycles of 30 s at 94 °C, 1 min at 50 °C and 2 min at 72 °C, and a final extension step of 10 min at 72 °C). The Promega Wizard® Genomic DNA Purification Kit (Version 12/2010) was used to purify the sequences from the above procedure. The 16S rRNA genetic fragments collected from the process above were aligned to reference sequences from other ar-omatic compound oxidizing organisms.

The data was analysed using the program BIOEDIT (Bioedit Ltd, Manchester Science Parks, Pencroft Way, Manchester, UK) to determine probabilities of closeness of evolutionally relationships. From the BIOEDIT Statistical Package, pairwise evolutionary dis-tances were computed based on an unambiguous stretch of 1274 bp using the method earlier outlined by Reller et al. (2007).

The DNA sequence from each culture was uploaded to the Basic Local Alignment Search Tool (BLAST) of the National Center for Biotechnology Information (NCBI). A neighbour-joining method in

the MEGA Version 6 software (Tamura et al., 2013) was used in conjunction with the data from BIOEDIT to construct the phylogenetic trees from the 16S rRNA sequence data.

2.4. Biosurfactants overproduction

Cells were harvested from different batches by centrifugation at 6000 rpm for 15 min under refrigeration (4 °C). In batch experiments, biosurfactant overproduction was performed prior to the degradation experiments. Harvested cells were inoculated in 30 L of mineral salt medium with composition of (g/L): 0.1 g $MgSO_4.7H_2O$, 4.5 g $Na_2HPO_4.2H_2O$, 0.68 g KH_2PO_4, 4.5 g $NaNO_3$ and 0.5 g yeast extract. 50 mL of sunflower oil was added to the medium as a carbon source. During the biosurfactant overproduction phase, 10 mL samples were collected from the production tank at 24 h intervals. Samples were analysed for surface tension using a Du Nouy tensiometer. The value of F in the Du Nouy test was inversely proportional to the amount of biosurfactant produced. In continuous flow experiments, biosurfactants overproduction was performed in the CSTR stage where biosurfactants producing conditions were maintained. Additionally, this phase was used for dissolution of PAHs before feeding the compounds to the biofilm reactor phase. The biofilm phase was designed to enhance biodegradability of the compounds taking advantage of the shielding effect of the concentration gradient on toxic exposure to cultures deeper into the biofilm.

2.5. Biosurfactant extraction

Crude biosurfactant was extracted and purified to enable further analysis of the chemical composition and structure later in this study. The biosurfactant extraction method was adopted from (Almeida et al., 2017). Produced biosurfactants solutions were centrifuged at 4 °C, 6000 rpm for 10 min. The pH of the cell free supernatant was adjusted from 8 to 2 using 3M HCl. A solution of chloroform:methanol (2:1v/v) was used to extract the biosurfactant. The process was performed three times to ensure high purity of the final product. The solvents were evaporated using a rotary evaporation. Based on these applied conditions, a biosurfactant purity of 80−85% was achieved during the processes of extraction and purification method using the chloroform/methanol extraction method described above (Bezza and Chirwa, 2016).

2.6. Biosurfactant characterisation

Biosurfactant molecular structure was determined by Fourier Transform Infra-Red spectrometry (FTIR) using instrument settings from earlier studies (Bezza and Chirwa, 2016, 2017). Physical characteristics were used to determine activity affinity for PAH surface. Physical characteristic measured include surface tension, emulsification index, and foaming. A chromatographic separation technique for the biosurfactant characterisation included the rudimentary Thin Layer Chromatography which was interpreted in conjunction with the FTIR results.

2.6.1. Surface tension

A Du Nouy tensiometer (Kruss Tensiometer, Model K11, Germany) was used to determine surface tension in culture inoculated media which was calibrated against the force exerted by a 1.9 cm lightweight platinum ring gently lowered onto a water surface. Killed culture medium and filtered (cell-free) media were used as baseline controls. For each sample, three independent measurements were taken at room temperature (25 °C) and the average value was recorded.

2.6.2. Emulsification index (E_{24})

E_{24} was determined as a percentage of the height of an emulsified layer to the total liquid column height following the method earlier developed by Bento et al. (2005). In the method, 5 mL cell free supernatant of the cultured sample was mixed with 5 mL of hexane (1:1 ratio), was mixed by stirring for 2 min and left to settle for 2 h to allow sufficient separation of the phases.

2.6.3. Foaming

The presence of foam was used as visual evidence of the presence of biosurfactant in the solution. Foam formation occurred when surfactants became concentrated at a gas-liquid interface, leading to formation of bubbles through the liquid and on the interface (Satpute et al., 2010). Excessive foaming is known to occur in mixtures containing lipoprotein biosurfactants such as surfactin due to the presence of hydrophilic amide moeities at the closing ends − tip of the lipid − of the surfactin molecule (Shaligram and Singhal, 2010). There were three stages of foaming observed consistent with the classifications indicated by Shaligram and Singhal (2010), i.e., (i) early foam characterised by low biomass and low mass transport in the system, (ii) stabilized stage foam characterised by green colour typical of *Pseusomonas aerignosa* culture, and (iii) death phase or starvation stage foam characterised by thick biomass with low viable cells and a brownish colour representing dying biomass. Fig. 1 shows foaming under (a) batch conditions, (b) during the mixing phase and (c) during the quiescent phase of the sequence-batch semi-continuous flow mixed reactor operated intermittently as a CSTR.

2.6.4. Thin Layer Chromatography

The chemical-interactive nature of the purified biosurfactant was determined using Thin Layer Chromatography (TLC). This method measures migration of compounds on a defined immobile phase. Mobile phases of biosurfactant drops were tracked on F_{254} plates (Merck Co. Inc., Damstadt, Germany) carried along by chloroform:methanol:water (65:25:4, by vol.) (Symmank et al., 2002). Plates with mobilised biosurfactant were then sprayed with water and air-dried in the presence of an ammonium molybdate-perchloric acid (AMPA). The AMPA solution was prepared from (a) 3 g $(NH_4)_2Mo$ in 25 mL deionised water, (b) 1 N HCl, and (c) 60% $HClO_4$ (Touchstone, 1992). The plates were then lightly heated to covert compounds into brown spots visible to the naked eye that were later quantified based on the extent of migration of the constituent compounds from initial drop deposition point.

2.6.5. Fourier Transform Infrared spectroscopy

The chemical structures and functional groups of around the crude extracted biosurfactant were characterised by the Fourier transform infrared (FTIR) spectroscopy (PerkinElmer 1600 Series FTIR, PerkinElmer, Waltham, Massachusetts, United States). The scans was conducted by an Attenuated Total Reflectance (ATR) Crystal Accessory from PerkinElmer. The range of the IR scan was set over 400−4000 cm^{-1} wavenumber with a resolution of 2 cm^{-1}. The reflectance spectra were recorded and averaged over 32 scans using the total internal reflectance configuration taking advantage of a Harrick™ MVP-PRO vaporiser. Spectra were viewed using the Spectrum 10TM software (PerkinElmer, Waltham, Massachusetts, USA).

2.7. PAH measurement by HPLC

PAHs were measured using a Waters 2695 HPLC equipped with a Waters PAH C_{18} column with the following specification: 250 mm × 4.6 mm × 5 μm, immobile phase (Waters Corporation). Compounds were detected by the Waters Photodiode Array
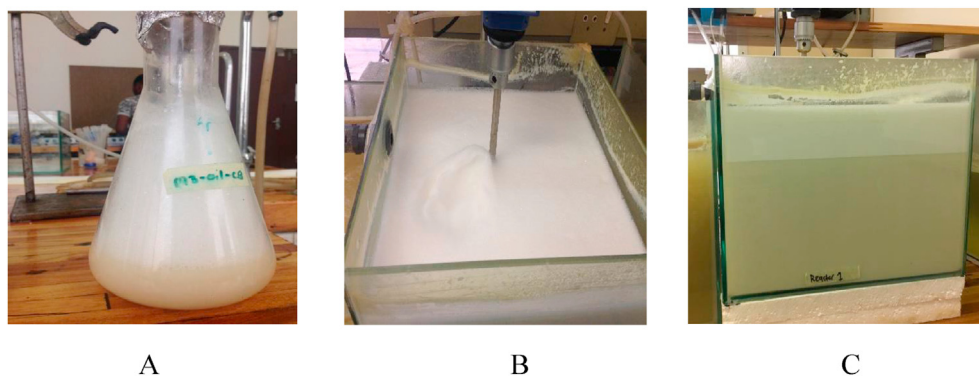
Fig. 1. Phase 1 - early foam - examples in batch (a) and continuously stirred tank reactor (CSTR) (b), and (c) Phase 2 - mature foam - in continuously stirred tank reactor.

Detector (PDA) Model 2998 detector (Waters Corporation, Massachusetts, USA). The system was operated at a near constant temperature of 25 °C and 4000 psi pressure. The detection wavelength was set at 254 nm. The sample was introduced on the column at 1 min sample analysis programme with a 70% acetonitrile, 30% ultrapure water mobile phase under isocratic conditions. A recovery cycle was applied with 100% ultra-pure water depending on the quality of subsequent chromatograms.

2.8. TOC analysis - biomineralisation

Total organic carbon (TOC) was measured using the Shimadzu 5000 TOC Analyser (Shimadzu, 1 Nishinokyo Kuwabara-cho, Nakagyo-ku, Kyoto 604−8511, Japan). Sodium thiosulphate mono

hydrate ($Na_2S_2O_3 \cdot H_2O$) was used as the COD standard for calibration of the instrument. Each standard was injected 3 times into the TOC Analyser and the result was only accepted if the coefficient variation ($CV = s/\overline{x} \times 100$) was less than 0.5%.

2.9. CSTR/biofilm reactor configuration

The continuous-flow CSTR/biofilm reactor system consisted of a 3 L biosurfactant dissolution zone, a feed stream of MSM, an 8 L CSTR tank (Reactor A) followed by a Fixed-Film Column (Reactor 2) for effluent polishing (Fig. 2). where biosurfactants were produced followed by feeding into a Pyrex glass column filled with 8 mm diameter ceramic beads with a liquid volume of 1.38 L and attachment surface area of 0.6760 m^3 (Fig. 2). The reactor system

1 – Dissolution tank

2 – Mineral Medium feed tank

3 – CSTR tank (Reactor 1)

4 – Overflow safety tank

5 – Biofilm column (Reactor B)

6 – Aeration and recycle bifurcation zone

7 – Effluent tank

Symbols

┴ Starring motor ▬ Connecting tubes 🔴 Pumps ● Pebbles for biofilm attachment
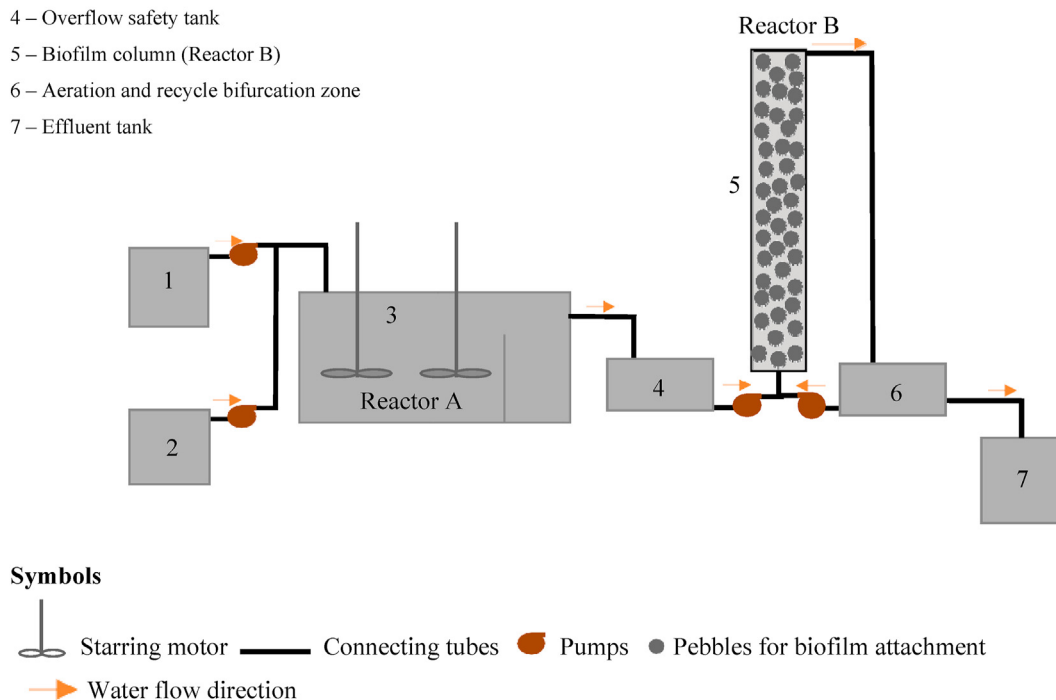
➤ Water flow direction

Fig. 2. Flow chart showing the preparation and feed zones (1 and 2), the main reactors Reactor A (CSTR) and Reactor B (Biofilm Reactor) and the Recycle and bifurcation zone (Zone 6).
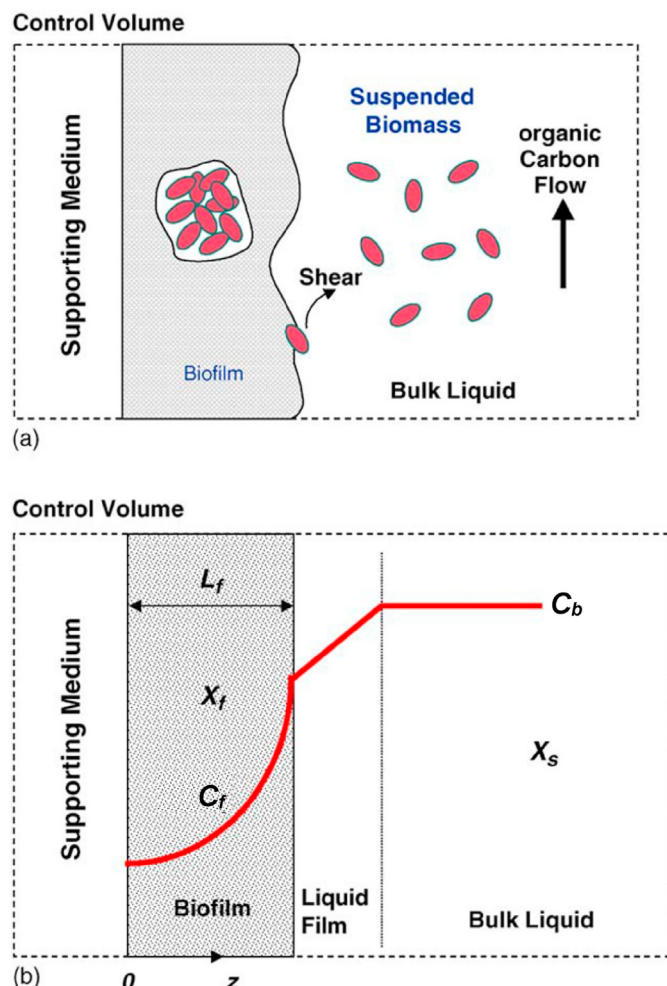
E.M. Nkhalambayausi Chirwa, T.B. Lutsinge-Nembudani, O.M. Fayemiwo et al.

Journal of Cleaner Production 290 (2021) 125183

Control Volume

Control Volume

Fig. 3. Biofilm model indicating (a) dynamic and mechanical factors affecting film thickness and density, i.e., attachment, growth and shear, and (b) kinetic factors affecting substrate removal, i.e., the diffusion-reaction process.

was operated under a hydraulic loading of 0.05 L/s ($\tau = 27.6$ h). The biofilm reactor was operated in counter-flow mode against gravity to ensure fully submerged conditions within the fixed media.

A tracer study was performed using a 100 mg/L NaCl feed solution to determine the flow and mixing regimes for dynamic modelling of the overall reactor system. Mixing regimes were evaluated at Q_R/Q_{in} values of 0, 1, 5, 10 and 20 for the fixed-film reactor. It was determined that at the recirculation rate of $Q_R/Q_{in} = 10$, the fixed-film reactor approached CSTR conditions. To ensure robust operation, a recirculation ratio (Q_R/Q_{in}) of 20 was used which also ensured that the column was adequately aerated from the bottom up.

2.10. Degradation kinetics of PAHs

From previous works, the biodegradation of LMW-PAHs in suspended growth cultures appeared to follow the Michaelis-Menten *mixed-order* kinetics (Chirwa and Wang, 2000). However, HMW-PAHs followed *first-order* kinetics due to the low dissolution rates and the low concentrations of the pollutant in the aquatic phase (Tikilili and Chirwa, 2011Tikilili and Chirwa, 2011). The combined generic kinetics can be best represented by the Monod kinetics (Eq. (1)):

$$\frac{dX}{dt} = Y\left(\frac{k_{mc}.C}{K_c + C}\right)X - k_d X \tag{1}$$

where C = substrate concentration ($M \cdot L^{-3}$), X = attached biomass density ($M \cdot L^{-3}$), μ_{max} = maximum substrate utilisation rate coefficient (T^{-1}), k_{mc} = substrate utilisation rate coefficient (T^{-1}), K_c = half-velocity coefficient ($M \cdot L^{-3}$), Y = cell yield coefficient ($M_x \cdot M_c^{-1}$), k_d = cell death rate coefficient (T^{-1}), and t = time (T). Depending on the magnitude of C relative to K_c, the reaction rate approaches *zero-order* kinetics at high values of C and *first-order* kinetics at very low values of C. Due to the relatively low solubility of PAHs in water, *first-order* degradation rate kinetics were adopted in Continuous Stirred Tank Reactors (CSTRs).

To model the movement and biodegradation of compounds across single-culture biofilm layers, the following assumptions
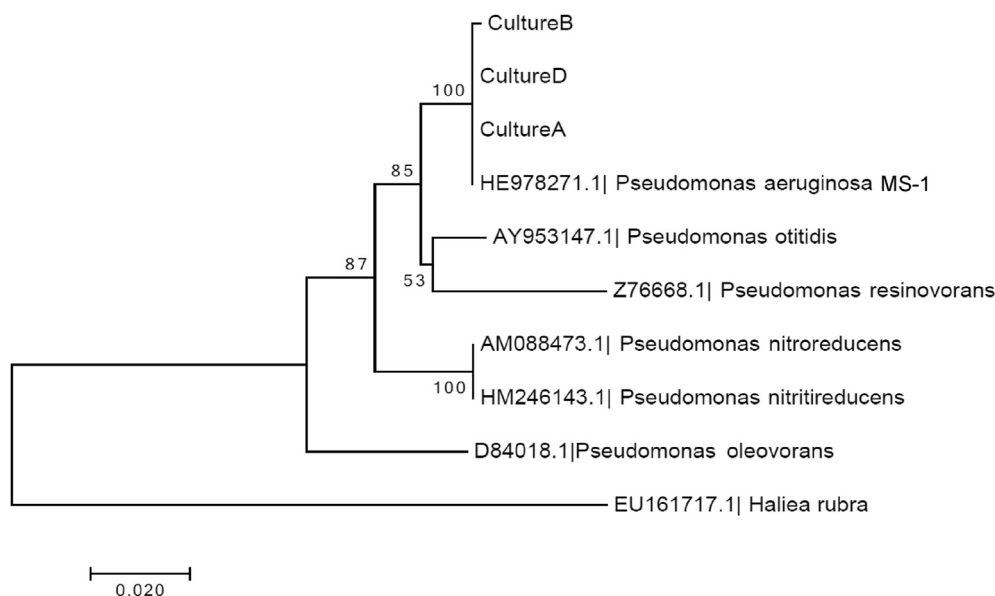

Fig. 4. Phylogenetic tree generated from the 16S rRNA genotype fingerprinting analysis of the Gram-positive colonies using *Haliea rubra* as an outgroup.

E.M. Nkhalambayausi Chirwa, T.B. Lutsinge-Nembudani, O.M. Fayemiwo et al.

Journal of Cleaner Production 290 (2021) 125183

Table 1
Surface tension of the media during biosurfactant overproduction.

Time (d)	0	1	2	3	4	6	8	9
Surface tension (mN/n)	62	53.69	50.09	42.13	30.89	28.34	28.09	27.82
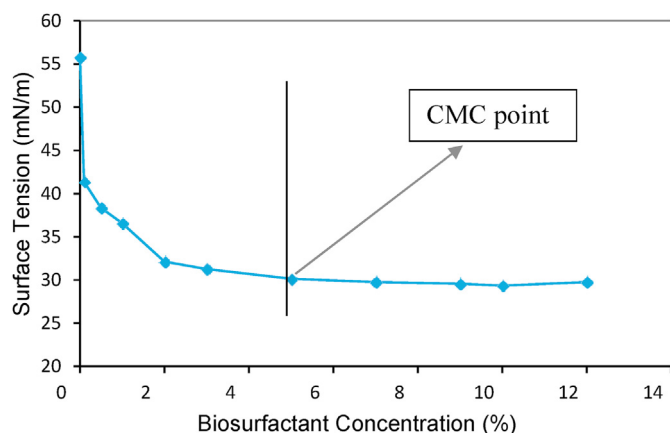
Fig. 5. The relationship between biosurfactant loading and surface tension reduction used to calculate the Critical Micelle Concentration (CMC).

were made based on earlier observations from Chirwa (1995): (1) for simplicity of modelling, the biofilm layer is assumed to be homogenous, (2) the support medium is assumed to be impermeable to water and soluble species such that all reaction occurs in the liquid medium and biofilm layer; (3) the stagnant liquid layer above the biofilm is so thin that removal of substances in this layer can be ignored; (4) the density of biofilm remains constant; (5) the increase in the biofilm thickness is due to microbial growth; (6) the substrate is transported from bulk liquid - liquid film - biofilm in the Z direction by molecular diffusion following the *Fick's law*; and (7) the internal biofilm dynamics is influenced by the values at the

boundaries — a boundary value problem (Fig. 3).

The mass transport of molecules through a *Newtonian Fluid* obeys *Fick's law* of molecular diffusion (Eq. (2)):

$$j_c = D_{cw} \frac{\partial C}{\partial z} \tag{2}$$

where D_{cw} = diffusion coefficient of C in water (L^2T^{-1}), j_c = flux rate across the liquid/biofilm interface ($ML^{-2}T^{-1}$). The removal of pollutants across the biofilm layer can thus be represented by the sum of diffusion and reaction rate kinetics (Chirwa and Wang, 2000):

$$D_f \frac{d^2 C_f}{dx^2} + r_i = 0 \tag{3}$$

where D_i = diffusion rate coefficient for the substrate C inside the biofilm (L^2T^{-1}), C_f = concentration (ML^{-3}) inside the biofilm at any depth x (L) from the surface. Eq. (3) is solved analytically only for first or zero order reaction kinetics of biological processes. The substrate volumetric conversion rate r_i is represented by the Monod form:

$$r_i = q_{max} \cdot \frac{C_f}{K_i + C_f} \cdot X \tag{4}$$

where q_{max} is the maximum specific substrate conversion rate ($ML^{-3}T^{-1}$), C_f is the substrate C concentration at the liquid layer/ biofilm interface (ML^{-3}), K_i is the affinity constant of substrate (ML^{-3}) and X is the attached biomass density (ML^{-3}). Simulations of the biofilm system under transient-state conditions solved numerically.
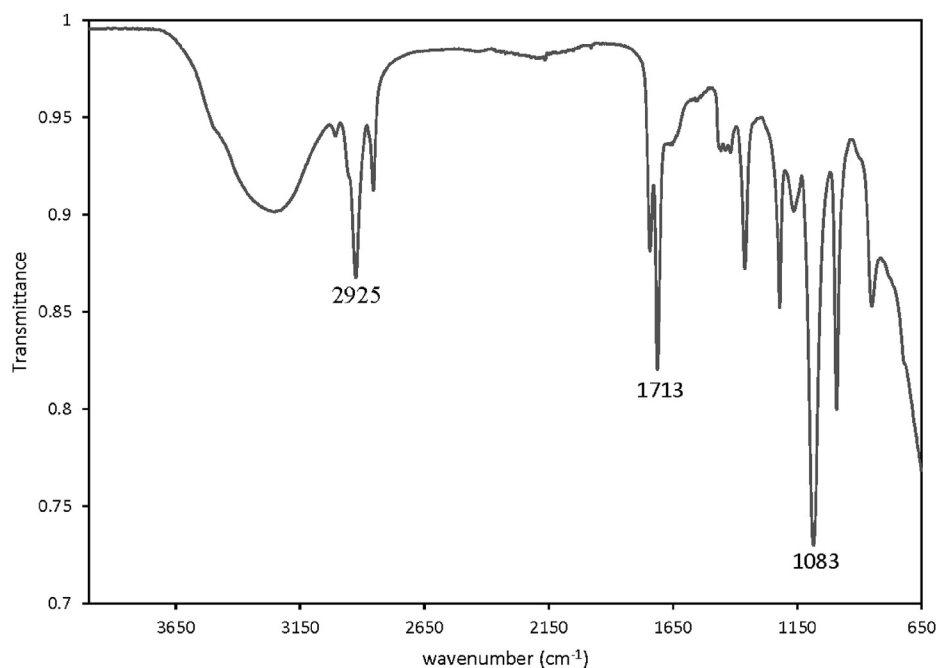

Fig. 6. FTIR performed on the purified harvested biosurfactant from the purified culture of *Pseudomonas aeruginosa* MS-1.
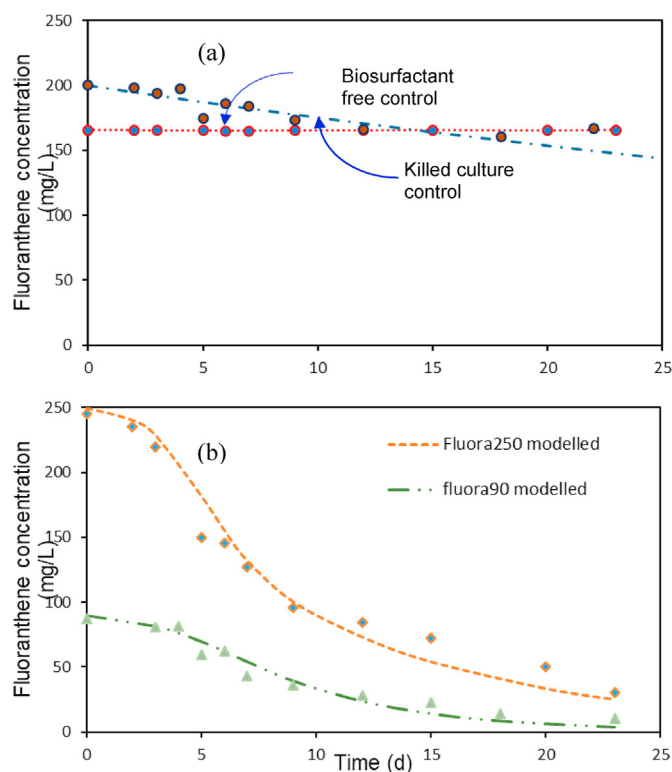
Fig. 7. Fluoranthene degradation in batch studies with kinetic modelled curves (a) kinetic degradation in cell free and killed culture controls, (b) first-order rate degradation at high (250 mg/L) and low (90 mg/L) flouranthene concentration using live cultures of *Pseudomonas aerigunosa* MS-1.
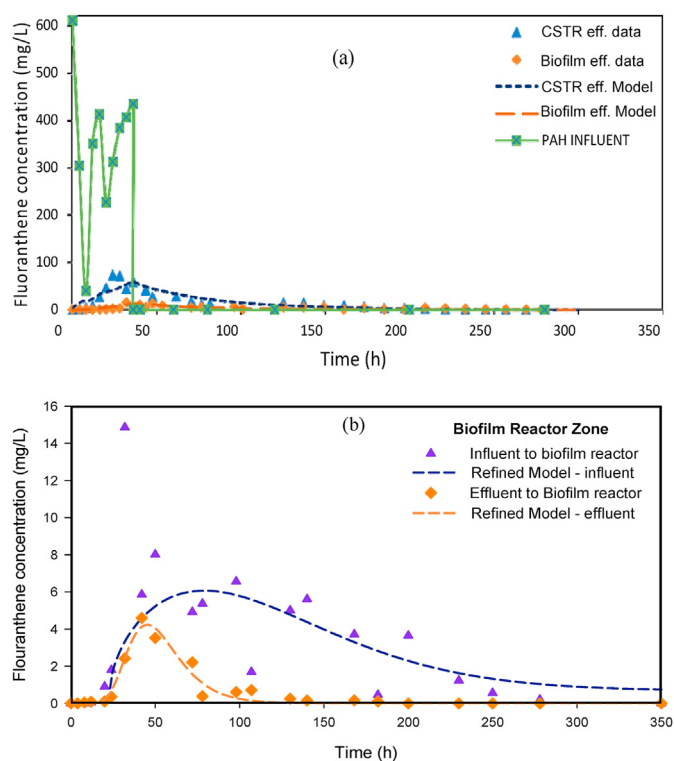

Fig. 8. Model fits for fluoranthene degradation in the continuous flow system from the CSTR reactor (Zone 2) and Biofilm reactor (Zone 3). (a) Is the initial reactor fit model representation for the two reactors in series, and (b) is the refined model for the measured effluent values from the two reactor systems.

Table 2
Batch kinetics parameter for mixed order fluoranthene degradation using *Pseudomonas aeruginosa* MS-1 showing a very high half velocity concentration (K_S) value relative to substrate concentration in the reactor.

Parameters	90 mg/L with biosurfactants	250 mg/L with biosurfactants
k_{max} (h^{-1})	0.236	0.295
K_S (mg/L)	992.01	991.84
CHI-Sqr (χ^2) (mg/L)^2	588	2213

3. Results and discussion

3.1. Species identification

The species identification results showed that the Samples A, B, and D belonged to members of genus Pseudomonas, with a 100% sequence similarity to *Pseudomonas aeruginosa* HE978271.1 [MS-1] (Fig. 4). Results in a preceding project (Dong et al., 2016), showed that pure cultures of a 100% homologs of *Acinetobacter junii* produced biosurfactant producing activity similar to observed activity in Samples A, B, and D from this study. Further analysis showed that the biosurfactants produced *A. junii* were structurally identical to bacterial rhamnolipid biosurfactants (Nie et al., 2010).

3.2. Biosurfactant characterisation

During biosurfactant overproduction, the surface tension of supernatants from different batches was measured periodically for 10−12 d. The data presented in Table 1 shows that, in the first 5 days of incubation, the surface tension dropped significantly from 60 mN/m to 27−29 mN/m. From day 6 and day 9, a slight decrease in surface tension was observed. In day 9, the surface tension

reached 27.82 mN/m, meaning that, the quantity of biosurfactants produced was sufficient to achieve the lowest possible surface tension to achieve dissolution and degradation of the PAHs. The above data showed that the biosurfactants produced were enough to cause the lowest possible surface tension. In surfactant reaction chemistry, the point of lowest surface tension is called the critical micelle concentration (CMC) (Fig. 5).

Thin Layer Chromatography (TLC) showed the appearance of a pink/brown spot on the silicon coated plate indicated a positive reaction. The pink/brown stain in the reagent used for TLC is a result of reaction with the peptide component of the lipoprotein biosurfactant. In the current case, the reagent used contained ninhydrin which turns brown in the presence of amino acids. From this initial phase, it was suggested that the extracted biosurfactant could be lipoprotein based. Figure S1 indicates a picture from the TLC test of the biosurfactants, used for dissolving fluoranthene and triphenylene.

Fourier Transform Infrared (FTIR) spectrometry was used to elucidate the predominant chemical functional groups in a purified crude biosurfactant sample (Fig. 6). Infrared absorption bands correspond to specific molecular components and structures in the scanned sample. The partially purified biosurfactant was analysed

Table 3
Critical kinetic parameters for simulation of fluoranthene degradation in the biofilm reactor under optimum temperature conditions.

Parameters	Description	Value
μ_{max} (h^{-1})	Maximum growth rate coefficient of cells in the biofilm zone	1.353
K_i (mg/L)	Specific inhibitive effect of fluoranthene in the bulk solution	30.899
D_i (m^2/h)	Optimum diffusion rate coefficient (Wicke et al., 2008)	3.6×10^{-6}
X (mg/L)	Bulk liquid cell concentration (measured)	230
Q (mg/m^3)	Influent hydraulic loading rate (measured)	8.63×10^{-4}
L_f (m)	Biofilm thickness [estimated (Kim and Cui, 2017)]	0.0005
EV%	Average model deviation from measured vales	3.8
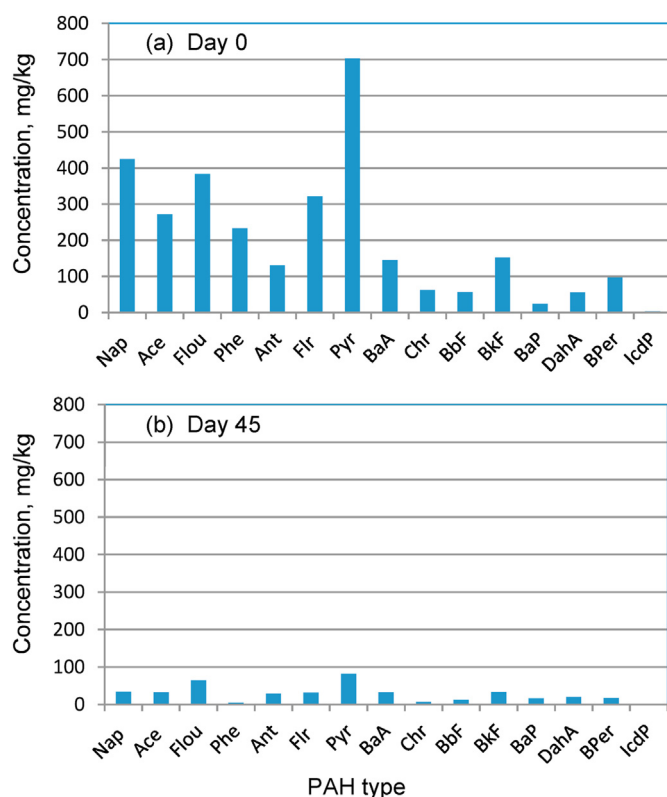
Fig. 9. Degradation of mixed PAHs in a creosote contaminated soil biopile over a 45 day period - creosote served as the source of PAHs in this samples. Fifteen(15) different PAH compounds were detected in the sample with ranging molecular weights from L- to HMW PAHs.

and the FTIR spectrum showed −NH- (peptide group) broad absorbance peak centred on 3264 cm^{-1} highly magnified above the expected OH$^-$ stretch, C−H (alkane group) sharp peak around 2925 cm^{-1}, C-ON (amide group) strong stretching mode peak around 1713 cm^{-1}, −CH$_3$,CH$_2$- (aliphatic chains) medium weak multiple bands from around 1457 to 1418 cm^{-1} and C−N (amine group) strong stretching mode peak around 1084 cm^{-1}. The biosurfactant structure shows a nominal OH^{-1} stretch a3400 cm^{-1} and the amide and −COOH peaks at 1713 and 1083 cm^{-1}, respectively. Many literature sources confirmed that the observed values were consistent with the abundance of lipoprotein biosurfactants in the samples (Fig. 6) (Coto and Arrondo, 2001; Krilov et al., 2009).

3.3. Fluoranthene degradation kinetics

3.3.1. Flouranthene degradation in batch reactors

Batch experiments were conducted using flouranthene as the test compound under enhanced solubility firstly with methanol as solvent and later using extracted biosurfactant. A purified culture of *P. aeruginosa* MS-1 was used as the biosurfactant producing agent. The *P. aeruginosa* MS-1 culture achieved 6.3% and 8.44% under 90 and 250 mg/L loadings, respectively. Abiotic activity observed in heat-killed cultures showed no PAH degradation showing that the observed PAH removal was metabolically linked (Fig. 7a). Live curves, on the other hand, showed a lag-phase of 3 days before Flouranthene was rapidly degraded in a logarithmic phase until the system stabilized at 18−20 days (Fig. 7b).

No significant degradation of flouranthene was observed in biosurfactant free controls and heat killed culture controls due to limited abiotic activity in these control b. After the fitting the model to experimental data, the optimum values of k_{max} and K_s were obtained as indicated in Table 2. The results from the 250 mg/L and 90 mg/L batches showed a higher rate at 250 mg/L, $k_{max} = 0.295$ d^{-1}, compared to only $k_{max} = 0.236$ d^{-1} at 90 mg/L which might be due to higher biomass at 250 mg/L.

3.3.2. Degradation kinetics in a dynamic CSTR/Biofilm reactor system

The base conditions in the reactors CSTR Reactor A and Biofilm Reactor B were assumed to be constant in a 2 day (48 h) range for modelling purposes. Further work is being conducted to achieve a *transient-state* model with continuously varying conditions in both reactors. Due to the slow dissolution rates of the PAH carbon sources, both the substrate utilisation rate and the biomass accumulation rate were represented by the *first-order* reaction rate dynamics. Fig. 8 presents a reactors in series model for the two reactor systems with a fixed-film reactor converted to a CSTR by applying a recirculation ration $Q_R/Q_{in} = 20$. In the CSTR operation mode, the kinetic model was simplified to a pseudo-first order model with $k_d \approx k_{max}/K_S = 0.00286$ d^{-1} [CHI-Sqr (χ^2) (mg/L)^2]. Other operational parameters relating to mass transport and operation conditions for the Biofilm system are presented in Table 3.

The model overestimated the CSTR output from 50 to 100 h operation. This could be due to the lower influent loading observed due to some blockages in influent tubing and other technical errors encountered. The increase in the retention/residential time in the system allowed longer contact time between the fluoranthene compounds and the biomass, which resulted in more fluoranthene degradation. After 100 h of the experimental run, the model underestimate the concentration of fluoranthene in the system. This could be due to the fact that there was almost no blockage of the tubes to decrease the flow.

In systems with lower or insufficient mixing, the mass transfer boundary layer thickness influence is large than the specific reaction rate at cell surfaces. The removal rate of the compound will then decrease due to the slow transportation of the compound from the bulk liquid to the cell. However if the mixing is great, the transfer boundary layer is eliminated which results in higher mass transport.
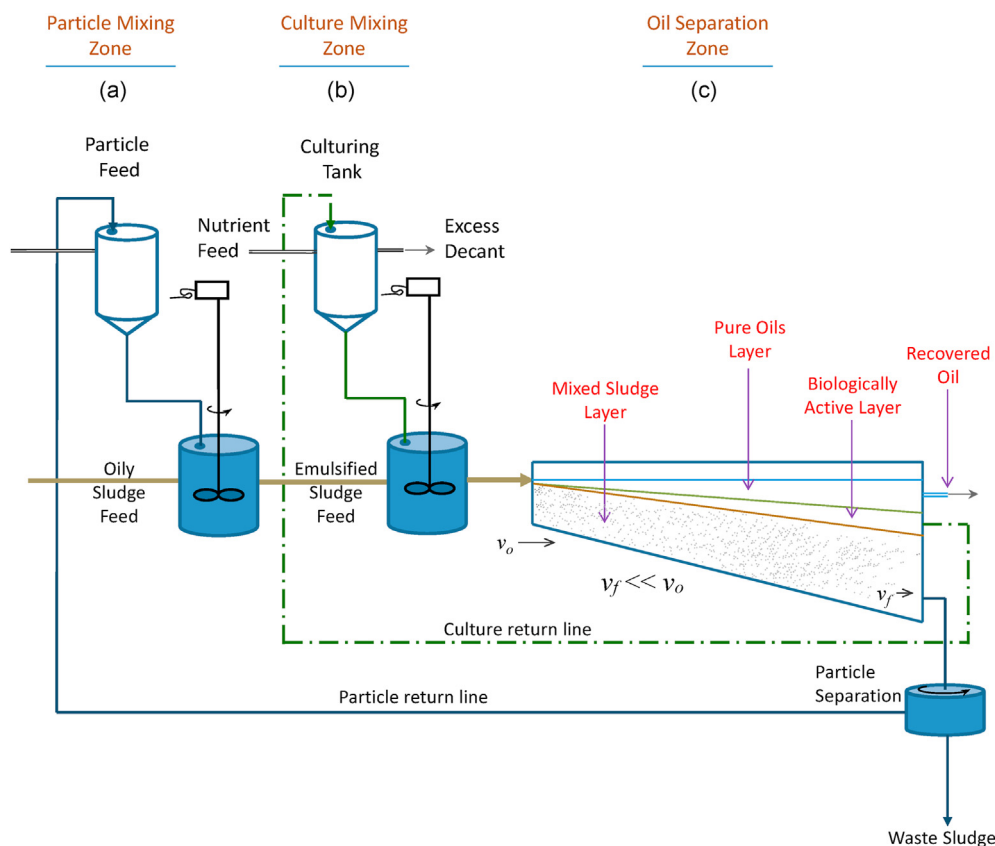
Fig. 10. The reactor schematic showing (a) 'Pickering' emulsion chamber, (b) demulsification chamber, and (c) oil separation fed-batch plug-flow zone. A further objective was to return solids for recycle into the 'Pickering' emulsion zone.

3.4. Purification of PAHs in biopiles and oil recovery systems

3.4.1. Biodegradation of PAHs in soil biopile

Experiments were conducted in both slurry and solid column biopile reactors using soil extracted for a creosote contaminated site in Pretoria (SA). PAH analysis was performed by a combination of methods targeting the immobile (diffused phase) and degradation rate in the aqueous state. The initial concentrations of PAHs is shown in Fig. 9a. A culture and spike of biosurfactants harvested at the log growth phase and was introduced in the reactor and the reactivity was measured.

Fig. 9a presents initial PAH concentration after dissolution by a biosurfactant soup, and Fig. 9b shows the measured concentration at 45 days (86% degraded). Each bar represents an average value from a quadruplicate sample analysis. LMW compounds occurred in abundance and the group that was most easily degraded (Fig. 9b). The lowest degradation efficiency was HMW compounds was benzo[a]pyrene (BaP) which achieved less than 5% degradation of the PAH substrate in 48 h.

3.4.2. Biodegradation of PAHs in recovered oily sludge - plug flow system

A system for oily recovery from oily sludge was developed based on an impact velocity reduction hypothesis in a tapered fed-batch plug-flow system (Fig. 10). This consisted of two mixing tanks, one for mixing the sludge and particles to achieve a "Pickering emulsion" with fumed silica particles, and the second chamber to receive culture and biosurfactant from a bioreactor chamber to start the demulsification process. The mixture with biosurfactant and culture was fed into the plug-flow phase, a 1.2 m long × 15 cm

plug flow gradient reactor with decreased particle velocity. The treated sludge mixture flow along the Plug Flow reactor was determined to be laminar flow. For this reason, longitudinal mixing of the sludge was not expected as it flowed along the laminar flow chamber.

3.4.3. Effects of water flooding during oil recovery

Fig. 11 shows the gains achieved in the oil recovery process using a semi-continuous fed-batch system (FB-PFR) system as an improvement over the simple batch system (Fig. 11a). Results show that the fed-batch plug-flow system achieved significantly higher oil recovery than the simple batch system within a defined time frame. In the batch system, mixing was poor therefore the sludge matrix where this was semi-solid remained stable. Additionally, the FB-PFR offered more operational flexibility such as varying the water content of sludge and biosurfactant exposure rate to an optimum value. In this system, it was shown that the oil recovery rate could be improved to 40% by adding biosurfactant producing bacteria with water over flooding (BSC + WF) (Fig. 11a). The FB-PFR system too advantage of the variable gradient in the plug-flow separation zone, which resulted in the slowing down and loss of energy in the fumed-silica particles as they travelled down the long variable-gradient reactor. Just like in any on the discrete particle dynamic systems, lighter particles in this system travelled further downstream than heavier particles thereby by facilitating more efficient separation of phases. The trend of accumulation of the oil over time approximates mixed-order kinetic with the mass approaching a q_{max} value of 46 mL·L^{-1} sludge. The results show that higher oil outputs were achieved with increased sludge loading velocities in the ranges tested thus far. Including the water
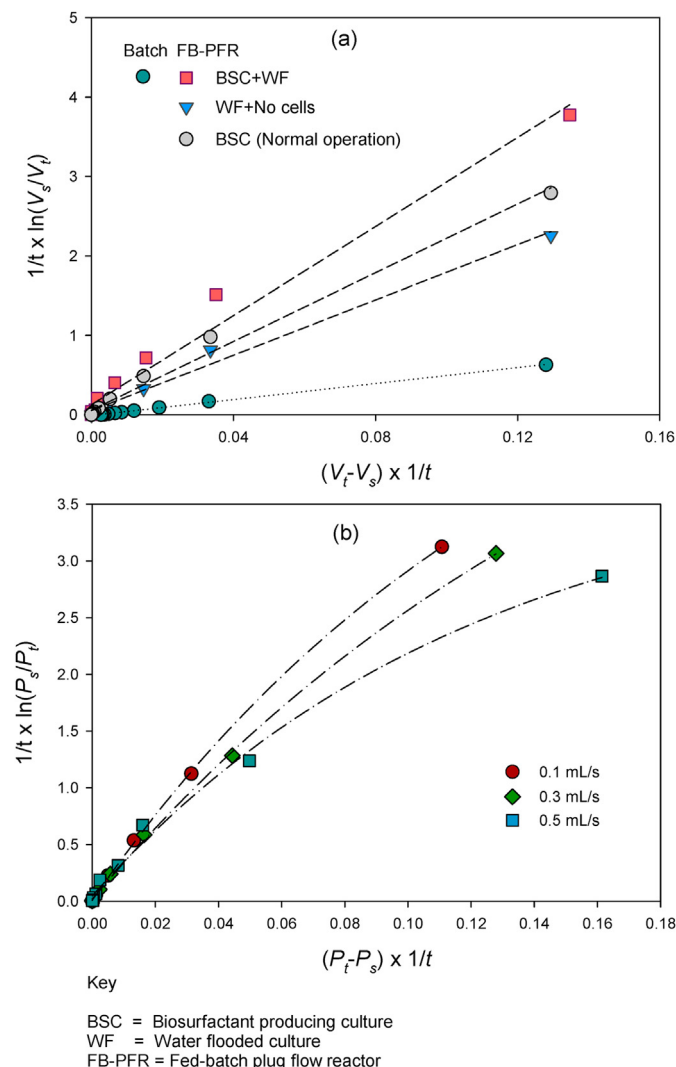
E.M. Nkhalambayausi Chirwa, T.B. Lutsinge-Nembudani, O.M. Fayemiwo et al.

Journal of Cleaner Production 290 (2021) 125183

Fig. 11. Results showing (a) improved performance of the FB-PFR systems compared to the batch systems under similar operational conditions, and (b) percent oil recovery as a percentage of oil determined in the original sludge mass.

Table 4
Oil accumulation rate parameter values under different operational conditions.

Parameters	Value	Operation Condition
k_{OL}/K_{OL} (units)	5.041	Batch
	17.410	PF - Water Flooding
	21.643	PF - Biosurfactant only
	28.042	PF - Water Flooding + Biosurf
EV%	2.23	PF - Water Flooding + Biosurf
q_{OL}/Q_{OL} (units)	28.042	PF - 0.1 mL/s
	18.011	PF - 0.3 mL/s
	12.566	PF - 0.5 mL/s
EV%	4.6	Average for all conditions

dosing − flooding − increased the oil recovery efficiency in both batch and FB-PFR systems (Fig. 11b). The accumulation of oil followed saturation-order kinetics indicated in Eq. (7) below. For volume of oil recovered at any time:

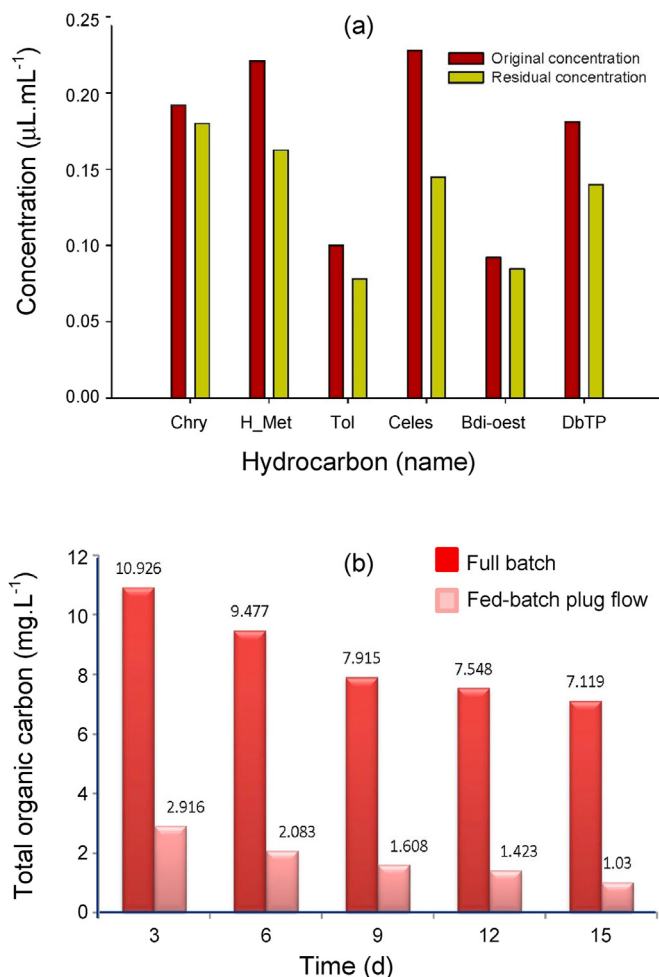$$\frac{dV}{dt} = \frac{k_{OL}V}{K_{OL}+V} \tag{7}$$

Fig. 12. (a) Degradability of representative PAHs identified in the sludge, i.e., chrysene (chry), 3-heptanone-4-methyl (H-met), toluene (Tol), celesticetin (Celes), 1, 2-benzene-di-iso-octyl ester (Bdi-oest) and Dibenzothiophene (DbTP), and (b) TOC content in the batch and FB-PFR treated sludge during storage and incubation at room temperature (25 °C) using only residual organisms within the waste solids.

where, V = volume of oil collected per litre of oily sludge, k_{OL} = oil accumulation rate coefficient and K_{OL} = saturation coefficient (mL·L^{-1}). The linearised saturation order kinetics show linear correlation of accumulation over time (Fig. 11a). And inverse correlation between loading rate and oil accumulation efficiency at different loading velocities (Fig. 11b). It is also shown that the relationship between loading and time become more and more non-linear with increasing loading rate (Fig. 11b).

The slope in the regression plots in Fig. 11a represent the variable k_{OL}/K_{OL} which is a measure of the rate of accumulation of oil under the different stipulated conditions. The reported change in k_{OL}/K_{OL} is mainly attributed to the change in K_{OL}. Ofter optimisation of the model, the value of k_{OL} did not change much. Increasing the loading rate of sludge into the reactor resulted in loss of efficiency in oil recovery (Table 4).

3.4.4. TOC residual analysis after oil recovery

The bottom effluent from the FB-PFR process (residual sludge) was stored in buckets for further treatment. The treatment entailed incubation at 30 °C for an additional 15 days with samples taken every 3 days. TOC analysis was performed on each sample to evaluate degradability of residual components.

The results obtained over a 15 day period (Fig. 12a&b) showed a clear improvement is quality in the FB-PFR system in comparison to

simple batch data. The material from simple batch residual yielded a mixture of organic material with low alkanes levels. The lower TOC observed in the residue (bottom flow) of the FB-PFR implies a higher TOC yield in the oil layer although this was not measured at this stage.

The results showed that compounds requiring more energy to degrade, i.e., simple hydrocarbon chains, were least likely to be degraded first (Fig. 12a&b). Complex aromatic compounds of the lowest entropy were degraded first. This process resulted in the conservation of the oil components in the residual sludge. It is therefore possible to reusable hydrocarbons during the biological process while degrading the unwanted polar aromatic compounds.

The decrease in TOC observed in the final residue was determined to be due to degradation of larger molecules in the sludge. The decrease in total organic carbon content with time (Fig. 12b) indicated further degradation of compounds to achieve a cleaner product for final disposal.

One of the most significant findings was that, the culture demonstrated selectivity between the alkanes and aromatic in the system. The culture of *Pseudomonas aeruginosa* MS-1 clearly preferred the aromatic constituents over the aliphatic alkanes probably due to the higher energy required to degrade the latter.

4. Conclusion

The study concluded that the purified culture of *Pseudomonas aeruginosa* MS-1 enhanced biosurfactant production and dissolution of High Molecular Weight Polycyclic Aromatic Hydrocarbon (HMW PAHs). In this study, fluoranthene was successfully degraded in batch with a pre-culture phase allowing dissolution to 200 mg/L followed by degradation in batch. The results show that culturing and sometimes harvesting the biosurfactant provide an opportunity to enhance biodegradability of these compounds. For future applications, it is demonstrated that a biofilm environment, due to its heterogeneity, enhances the survival of the biosurfactant producing and PAH degrading organisms resulting in a higher performance of the cultures in a continuous flow biofilm system. A kinetic modelling approach showed that mass transport resistance can play role in delaying the toxic effects of PAHs on cells through mass transport resistance shielding. The biofilm reactor system achieved 98% efficiency in removing IMW to HMW PAHs, much higher than PAH removals in suspended culture CSTR and batch culture systems.

5. Credit author statement

The submitting author declares that all authors listed in the paper contributed actively in the execution of the research project and participated in the generation of content on which this paper is based.

Declaration of competing interest

The authors declare that they have no known competing financial interests or personal relationships that could have appeared to influence the work reported in this paper.

Acknowledgement

Appendix A. Supplementary data

Supplementary data to this article can be found online at https://doi.org/10.1016/j.jclepro.2020.125183.

Funding

References

Abdel-Shafy, H.I., Mansour, M.S., 2016. A review on polycyclic aromatic hydrocarbons: source, environmental impact, effect on human health and remediation. Egyptian Journal of Petroleum 25 (1), 107–123.

Almeida, D.G., Soares da Silva, R.d.C.F., Luna, J.M., Rufino, R.D., Santos, V.A., Sarubbo, L.A., 2017. Response surface methodology for optimizing the production of biosurfactant by *Candida tropicalis* on industrial waste substrates. Front. Microbiol. 8 (2017) https://doi.org/10.3389/fmicb.2017.00157.

Bamforth, S.M., Singleton, I., 2005. Bioremediation of polycyclic aromatic hydrocarbons: current knowledge and future directions. J. Chem. Technol. Biotechnol. 80 (7), 723–736.

Banat, I.M., 1995. Biosurfactants production and possible uses in microbial enhanced oil recovery and oil pollution remediation: a review. Bioresour. Technol. 51 (1), 1–12.

Benincasa, M., 2007. Rhamnolipid produced from agroindustrial wastes enhances hydrocarbon biodegradation in contaminated soil. Curr. Microbiol. 54 (6), 445–449.

Bento, F.M., de Oliveira Camargo, F.A., Okeke, B.C., Frankenberger Jr., W.T., 2005. Diversity of biosurfactant producing microorganisms isolated from soils contaminated with diesel oil. Microbiol. Res. 160 (3), 249–255.

Bezza, F.A., Chirwa, E.M.N., 2016. Biosurfactant-enhanced bioremediation of aged polycyclic aromatic hydrocarbons (PAHs) in creosote contaminated soil. Chemosphere 144 (February 2016), 635–644.

Bezza, F.A., Chirwa, E.M.N., 2017. The role of lipopeptide biosurfactant on microbial remediation of aged polycyclic aromatic hydrocarbons (PAHs)-contaminated soil. Chem. Eng. J. 309 (1 February 2017), 563–576.

Bodour, A.A., Miller-Maier, R.M., 1998. Application of a modified drop-collapse technique for surfactant quantitation and screening of biosurfactant-producing microorganisms. J. Microbiol. Methods 32 (3), 273–280.

Cachada, A., Coelho, C., Gavina, A., Dias, A., Patinha, C., Reis, A., da Silva, E.F., Duarte, A., Pereira, R., 2018. Availability of polycyclic aromatic hydrocarbons to earthworms in urban soils and its implications for risk assessment. Chemosphere 191 (January 2018), 196–203.

Cachada, A., Dias, A.C., Reis, A.P., da Silva, E.F., Pereira, R., Duarte, A.d.C., Patinha, C., 2019. Multivariate analysis for assessing sources, and potential risks of polycyclic aromatic hydrocarbons in lisbon urban soils. Minerals 9. https://doi.org/10.3390/min9030139.

Chang, J.S., Cha, D.K., Radosevich, M., Jin, Y., 2015. Effects of biosurfactant-producing bacteria on biodegradation and transport of phenanthrene in subsurface soil. Journal of Environmental Science and Health - Part A Toxic/Hazardous Substances and Environmental Engineering 50 (6), 611–616.

Chen, Y., Zhao, R., Xue, J., Li, J., 2013. Generation and distribution of PAHs in the process of medical waste incineration. Waste Manag. 33 (5), 1165–1173.

Chirwa, E., 1995. Hexavalent Chromium Reduction by Pure Cultures of *Bacillus Sp.* And *Pseudomonas Fluorescens* LB300 in a Fixed-Film Bioreactor. University of Kentucky, Lexington, Kentucky, USA, p. 1995.

Chirwa, E., Mampholo, T., Fayemiwo, O., 2013. Biosurfactants as demulsifying agents for oil recovery from oily sludge—performance evaluation. Water Sci. Technol. 67 (12), 2875–2881.

Chirwa, E.N., Wang, Y.-T., 2000. Simultaneous chromium (VI) reduction and phenol degradation in an anaerobic consortium of bacteria. Water Res. 34 (8), 2376–2384.

Chirwa, E.M.N., Mampholo, C.T., Fayemiwo, O.M., Bezza, F.A., 2017. Biosurfactant assisted recovery of oil and C11-C15 hydrocarbon preservation in a biological oil recovery process from oily sludge. J. Environ. Manag. 196 (July 2017), 261–269.

Chirwa, E.M.N., Makgato, S.S., Tikilili, P.V., Lutsinge, T.B., 2018. Bioremediation of chlorinated and aromatic petrochemical pollutants in multi-phase media and oily sludge. In: Bharagava, R.N. (Ed.), Environmental Pollution and Mitigation,

E.M. Nkhalambayausi Chirwa, T.B. Lutsinge-Nembudani, O.M. Fayemiwo et al.

Journal of Cleaner Production 290 (2021) 125183

Chap. 16. CRC Press, New York, NY, USA, ISBN 978-0-8153-8314-7, pp. 367–384.

Coto, X., Arrondo, J.L.R., 2001. Infrared spectroscopy of lipoproteins. In: Pifat-Mrzljak, Greta (Ed.), Supramolecular Structure and Function, vol. 7. Springer Nature Switzerland AG, pp. 75–87.

Das, N., Chandran, P., 2011. Microbial degradation of petroleum hydrocarbon contaminants: an overview. Biotechnology Research International 2011, 941810.

Dhote, M., Juwarkar, A., Kumar, A., Kanade, G.S., Chakrabarti, T., 2010. Biodegradation of chrysene by the bacterial strains isolated from oily sludge. World J. Microbiol. Biotechnol. 26 (2), 329–335.

Dong, H., Xia, W., Dong, H., She, Y., Zhu, P., Liang, K., Zhang, Z., Liang, C., Song, Z., Sun, S., 2016. Rhamnolipids produced by indigenous Acinetobacter junii from petroleum reservoir and its potential in enhanced oil recovery. Front. Microbiol. 7 (7 November 2016) https://doi.org/10.3389/fmicb.2016.01710.

Fayemiwo, O.M., 2015. Microbial Enhanced Oil Recovery from Oily Sludge Using a Novel Plug Flow Reactor System. Masters Dissertation, Department of Chemical Engineering, University of Pretoria. Available on line @. http://hdl.handle.net/2263/43335. Last accessed on 17 October 2020, 13:50.

Gan, S., Lau, E., Ng, H., 2009. Remediation of soils contaminated with polycyclic aromatic hydrocarbons (PAHs). J. Hazard Mater. 172 (2–3), 532–549.

Gidudu, B., Chirwa, E., 2019. Biosurfactant facilitated emulsification and electro-osmotic recovery of oil from petrochemical contaminated soil and oily sludge. Chemical Engineering Transactions 74 (2019), 1297–1302.

Gidudu, B., Chirwa, E.M.N., 2020a. Biosurfactants as demulsification enhancers in bio-electrokinetic remediation of petroleum contaminated soil. Process Saf. Environ. Protect. 143 (November 2020), 332–339.

Gidudu, B., Chirwa, E.M.N., 2020b. Approaching electrodes configurations in bio-electrokinetic deoiling of petrochemical contaminated soil. J. Clean. Prod. 276 (10 December 2020), 122745.

Kim, M., Cui, F., 2017. Use of Nonsteady-state Biofilm Model to characterize heterotrophic and autotrophic biomass within aerobic granules. KSCE Journal of Civil Engineering 21 (7 March 2017), 2584–2589.

Krilov, D., Balarin, M., Kosović, M., Gamulin, O., Brnjas-Kraljević, J., 2009. FT-IR spectroscopy of lipoproteins—a comparative study. Spectrochim. Acta Mol. Biomol. Spectrosc. 73 (4), 701–706.

Lasota, J., Błońska, E., 2018. Polycyclic aromatic hydrocarbons content in contaminated forest soils with different humus types. Water Air and Soil Pollution 229 (6), 204–212.

Li, A., Zhaoxu, X., Huijuan, Z., Qu, L.J., 2011. Characteristic transformation of humic acid during photoelectrocatalysis process and its subsequent disinfection byproduct formation potential. Water Res. 45 (18), 6131–6140.

Malá, J., Cvikrová, M., Hrubcová, M., Máchová, P., 2013. Influence of vegetation on phenolic acid contents in soil. J. For. Sci. 59 (7), 288–294.

Marchut-Mikolajczyk, O., Drożdżyński, P., Pietrzyk, D., Antczak, T., 2018. Biosurfactant production and hydrocarbon degradation activity of endophytic bacteria isolated from Chelidonium majus L. Microb. Cell Factories 17, 171. https://doi.org/10.1186/s12934-018-1017-5.

Nie, M., Yin, X., Ren, C., Wang, Y., Xu, F., Shen, Q., 2010. Novel rhamnolipid biosurfactants produced by a polycyclic aromatic hydrocarbon-degrading bacterium Pseudomonas aeruginosa strain NY3. Biotechnol. Adv. 28 (5), 635–643.

Patowary, K., Kalita, M.C., Deka, S., 2015. Degradation of polycyclic aromatic hydrocarbons (PAHs) employing biosurfactant producing Pseudomonas aeruginosa

KS3. Indian J. Biotechnol. 14 (April 2015), 208–215.

Reller, L.B., Weinstein, M.P., Petti, C.A., 2007. Detection and identification of microorganisms by gene amplification and sequencing. Clin. Infect. Dis. 44 (8), 1108–1114.

Rice, E.W., Baird, R.B., Eaton, A.D., 2005. Standard Methods for the Examination of Water and Wastewater - Centennial Edition.. American Public Health Association, American Water Works Association, Water Environment Federation, USA.

Sarma, P.M., Bhattacharya, D., Krishnan, S., Banwari Lal, B., 2004. Degradation of polycyclic aromatic hydrocarbons by a newly discovered enteric bacterium, Leclercia adecarboxylata. Appl. Environ. Microbiol. 70 (5), 3163–3166.

Sato, M., Tojo, Y., Matsuo, T., Matsuto, T., 2011. Investigation of polycyclic aromatic hydrocarbons (PAHs) content in bottom ashes from some Japanese waste incinerators and simple estimation of their fate in landfill. Sustainable Environmental Research 21 (4), 219–227.

Satpute, S.K., Banpurkar, A.G., Dhakephalkar, P.K., Banat, I.M., Chopade, B.A., 2010. Methods for investigating biosurfactants and bioemulsifiers: a review. Crit. Rev. Biotechnol. 30 (2), 127–144.

Shaligram, N.S., Singhal, R.S., 2010. Surfactin — a review on biosynthesis, fermentation, purification and applications. Food Technol. Biotechnol. 48 (2), 119–134.

Shokouhfard, M., Kermanshahi, R.K., Shahandashti, R.V., Feizabadi, M.M., Teimourian, S., 2015. The inhibitory effect of a Lactobacillus acidophilus derived biosurfactant on biofilm producer Serratia marcescens. Iranian Journal of Basic Medical Sciences 18 (10), 1001–1007.

Singer, P.C., 1999. Humic substances as precursors for potentially harmful disinfection by-products. Water Sci. Technol. 40 (9), 25–30.

Symmank, H., Franke, P., Saenger, W., Bernhard, F., 2002. Modification of biologically active peptides: production of a novel lipohexapeptide after engineering of Bacillus subtilis surfactin synthetase. Protein Eng. 15 (11), 913–921.

Tamura, K., Stecher, G., Peterson, D., Filipski, A., Kumar, S., 2013. MEGA6: molecular evolutionary genetics analysis version 6.0. Mol. Biol. Evol. 30 (12), 2725–2729.

Tikilili, P.V., Chirwa, E.M.N., 2011. Characterization and biodegradation of Polycyclic Aromatic Hydrocarbons in radioactive wastewater. Journal of Hazardous Materials 192 (3), 1589–1596. https://doi.org/10.1016/j.jhazmat.2011.06.079.

Touchstone, J.C., 1992. Practice of Thin Layer Chromatography. John Wiley & Sons, London, UK.

Tudoran, M., Putz, M., 2012. Polycyclic aromatic hydrocarbons: from in cerebro to in silico eco-toxicity fate. Chemical Bulletin of "Politehnica" University of Timisoara 57 (71), 50–53. Romania.

Ukiwe, L.N., Egereonu, U.U., Njoku, P.C., Nwoko, C.I., Allinor, J.I., 2013. Polycyclic aromatic hydrocarbons degradation techniques. Int. J. Chem. 5 (4), 43–55.

Vidali, M., 2001. Bioremediation: an overview. Pure Appl. Chem. 73 (7), 1163–1172.

Wheatley, A., Sadhra, S., 2004. Polycyclic aromatic hydrocarbons in solid residues from waste incineration. Chemosphere 55 (5), 743–749.

Wicke, D., Böckelmann, U.T.A, Reemtsma, T., 2008. Environmental Influences on the Partitioning and Diffusion of Hydrophobic Organic Contaminants in Microbial Biofilms. Environmental Science and Technology 42 (6), 1990–1996. https://doi.org/10.1021/es702267s.

Zhong, X., Cui, C., Yu, S., 2017. The determination and fate of disinfection by-products from ozonation-chlorination of fulvic acid. Environ. Sci. Pollut. Control Ser. 24, 6472–6480.